Lawrence Berkeley National Laboratory
Recent Work

Title
ENERGY RESOLUTION IN CYCLOTRON EXPERIMENTS

Permalink
https://escholarship.org/uc/item/35f4r0kh

Authors
Moss, Joel
Ball, Gordon C.

Publication Date
1966-09-01

eScholarship.org Powered by the California Digital Library
University of California

UCRL-17124

University of California
Ernest O. Lawrence Radiation Laboratory

TWO-WEEK LOAN COPY

This is a Library Circulating Copy which may be borrowed for two weeks. For a personal retention copy, call Tech. Info. Division, Ext. 5545

ENERGY RESOLUTION IN CYCLOTRON EXPERIMENTS

Berkeley, California

DISCLAIMER

This document was prepared as an account of work sponsored by the United States Government. While this document is believed to contain correct information, neither the United States Government nor any agency thereof, nor the Regents of the University of California, nor any of their employees, makes any warranty, express or implied, or assumes any legal responsibility for the accuracy, completeness, or usefulness of any information, apparatus, product, or process disclosed, or represents that its use would not infringe privately owned rights. Reference herein to any specific commercial product, process, or service by its trade name, trademark, manufacturer, or otherwise, does not necessarily constitute or imply its endorsement, recommendation, or favoring by the United States Government or any agency thereof, or the Regents of the University of California. The views and opinions of authors expressed herein do not necessarily state or reflect those of the United States Government or any agency thereof or the Regents of the University of California.

UCRL-17124
UC-28 Particle Accel.
and High Volt. Mach.
TID-4500 (49th Ed.)

UNIVERSITY OF CALIFORNIA

Lawrence Radiation Laboratory
Berkeley, California

AEC Contract No. W-7405-eng-48

ENERGY RESOLUTION IN CYCLOTRON EXPERIMENTS

Joel Moss and Gordon C. Ball

September 1966

Printed in USA. Price $2.00. Available from the Clearinghouse for Federal Scientific and Technical Information, National Bureau of Standards, U. S. Department of Commerce, Springfield, Virginia.

ENERGY RESOLUTION IN CYCLOTRON EXPERIMENTS*

Joel Moss and Gordon C. Ball

Lawrence Radiation Laboratory
University of California
Berkeley, California

September 1966

Abstract

An analysis was made of the factors affecting energy resolution in experiments carried out at the Berkeley 88" cyclotron. The contributions from various sources are treated individually and a method of combining these effects to obtain the total theoretical energy resolution is discussed. Good agreement was obtained when the theoretical calculations were compared with experimental results.

---

*This work was performed under the auspices of the U. S. Atomic Energy Commission.

Introduction

In cyclotron experiments it is important to know the factors affecting the energy resolution which is experimentally observed. This knowledge is necessary in order to optimize conditions for a given experiment and is essential if further improvement in energy resolution is desired.

The factors contributing to the energy resolution can be divided into two general categories: those which depend upon the quality of the analyzed beam and those which depend upon the apparatus used in studying a particular nuclear reaction. These factors are summarized in Table 1 and are discussed individually in Section II.

The quality of the beam which enters the target chamber is primarily determined by the source characteristics of the unanalyzed beam and the beam analysis system. The source is the region from which particles would appear to originate if one could look up the beam axis towards the cyclotron. Generally there will be two sources corresponding to the vertical and horizontal motion of the particles. A source can be specified by its position, width, and the maximum angle of divergence of the emerging particles.

Another important quantity to be considered is the dispersion or energy spread of the unanalyzed beam. Since the turn separation at the extraction radius is very small the cyclotron deflector intercepts several orbits of internal beam. Therefore, the unanalyzed beam contains particle energies distributed over a small range. To reduce this energy spread it is necessary to magnetically analyze the beam with a bending magnet. A more detailed discussion of this effect is presented in Section IIA-1.

The positioning of external bending and quadrupole magnets which are used to analyze and focus the beam is governed by the source characteristics and must be arranged to give the optimum beam at the target position. Ideally one would like to have a narrow and nearly parallel beam.

The experimental apparatus used in cave I has been discussed elsewhere[1] and is shown in Fig. 1. Figure 2 shows a schematic diagram of the optical system indicating the vertical and horizontal foci. The magnet currents necessary to obtain the desired foci were determined by an analog computer. The overall magnification of the optical system from the source to the target was calculated to be 3.1 in the horizontal plane. For a more complete treatment of beam optics the reader is referred to a book by J. Livingood[2] and an unpublished chemistry note by Bernard G. Harvey[3].

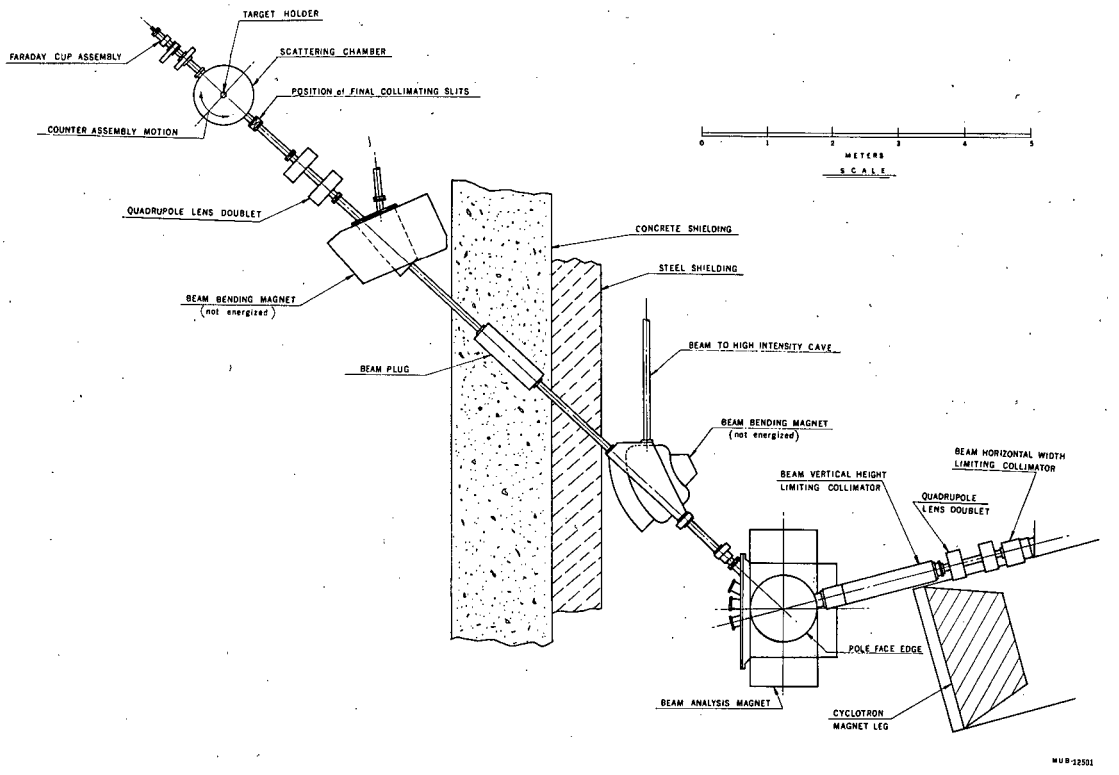

Fig. 1. The arrangement of experimental equipment for Cave I at the 88" cyclotron.

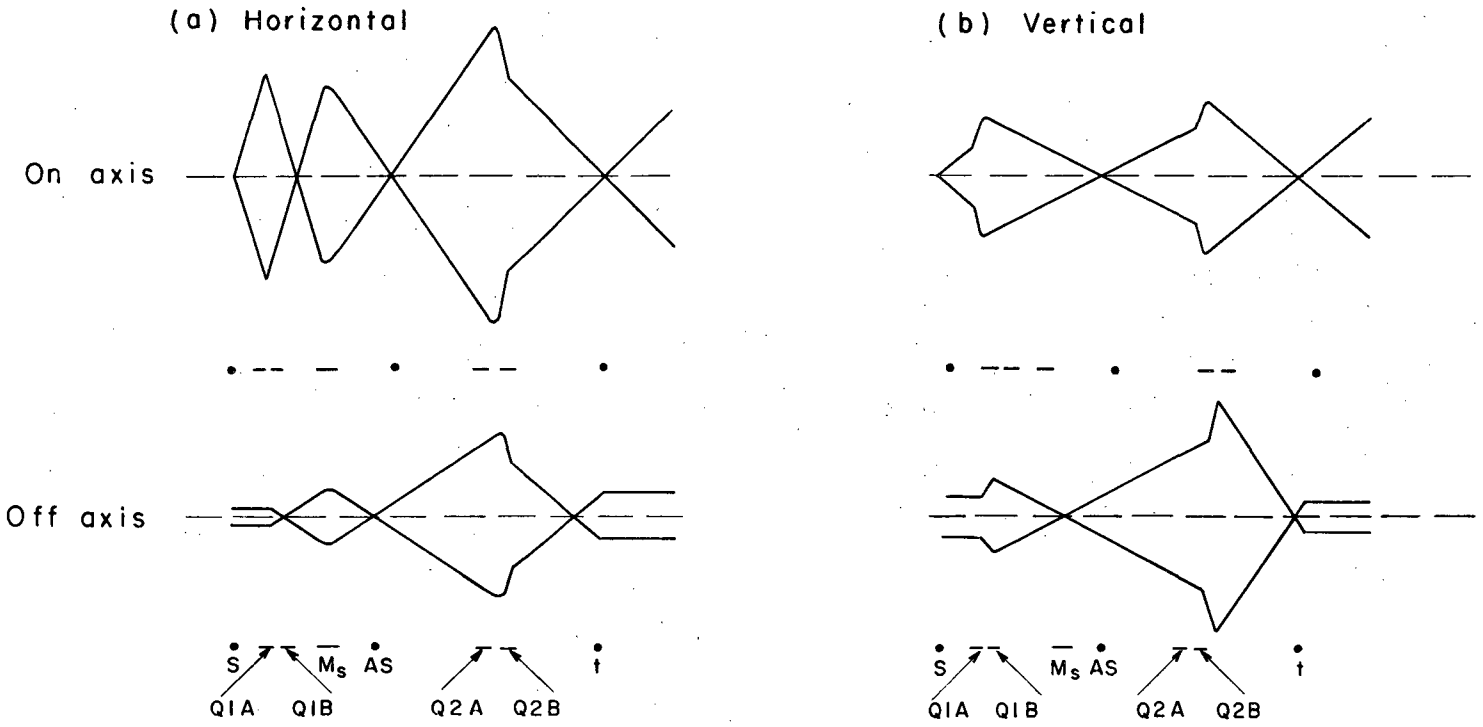

Fig. 2. The beam optical system in the horizontal (a) and vertical (b) planes where Q1A, Q1B, Q2A, and Q2B are the focusing elements of the quadrupoles 1 and 2 respectively, M_S is the bending magnet and S, AS and t are the positions of the source, analyzing slit and the target.

TABLE 1

Individual Contributions to Energy Resolution

	Angular Dependence	Shape of Resulting Peak
A. Beam Quality		
1. Analyzed Beam	No	Gaussian
2. Beam Convergence	Yes	Rectangular
3. Beam Width	Yes	Rectangular
B. Target and Detector Geometry Effects		
1. Solid Target		
a. Collimator Slit Width	Yes	Rectangular
b. Target Thickness	Yes	Rectangular
2. Gas Target Collimator Slit Widths	Yes	Triangular
C. Energy Straggling	No	Gaussian
D. Multiple Scattering	Yes	Gaussian
E. Electronic Noise	No	Guassian

I. The Relationship Between Angular Effects and Energy Resolution

The energy of the detected particles in a reaction or scattering experiment depends on the angle of detection measured from the beam axis (see tables 2, 3). Therefore, any effect which produces an angular spread $\Delta\psi$ in the particles detected causes an energy spread which is given by

$$\Delta E = \left(\frac{dE}{d\theta}\right)_{\theta_o} \Delta\psi \qquad 1.$$

where θ_o is the mean laboratory scattering angle.

If the detectors are located in the horizontal plane[1], angular effects in the vertical plane should be negligible; this may be seen from the following consideration. The scattering angle θ can be related to its components in the vertical (ρ) and horizontal (α) planes by the relationship (see Fig. 3)

$$\cos\theta = \cos\alpha \cos\rho \qquad 2.$$

If we consider an angular spread of $\Delta\rho = 1°$ then the change in the scattering angle $\Delta\theta$ for any angle α is shown in Fig. 4. Since the vertical effects are expected to be comparable to the horizontal ones, it is obvious from Fig. 4 that they may be neglected for scattering angles $\theta=\alpha > 5°$.

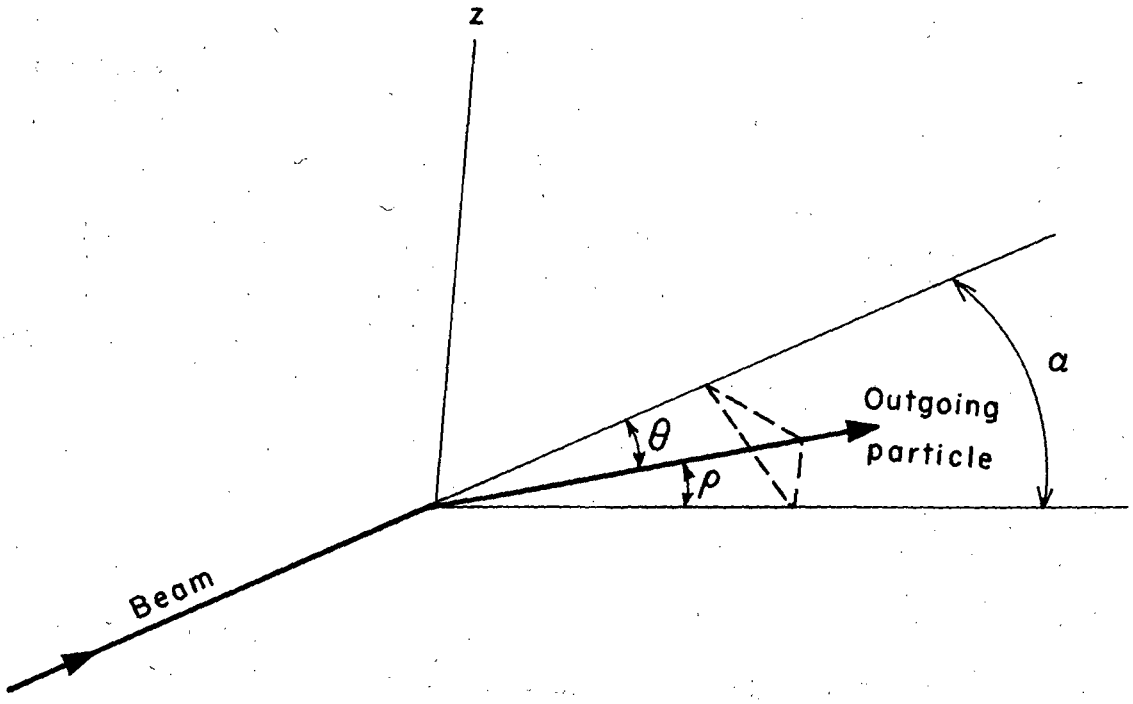

MUB-12742

Fig. 3. The scattering angle θ and its components in the vertical (ρ) and horizontal (α) planes.

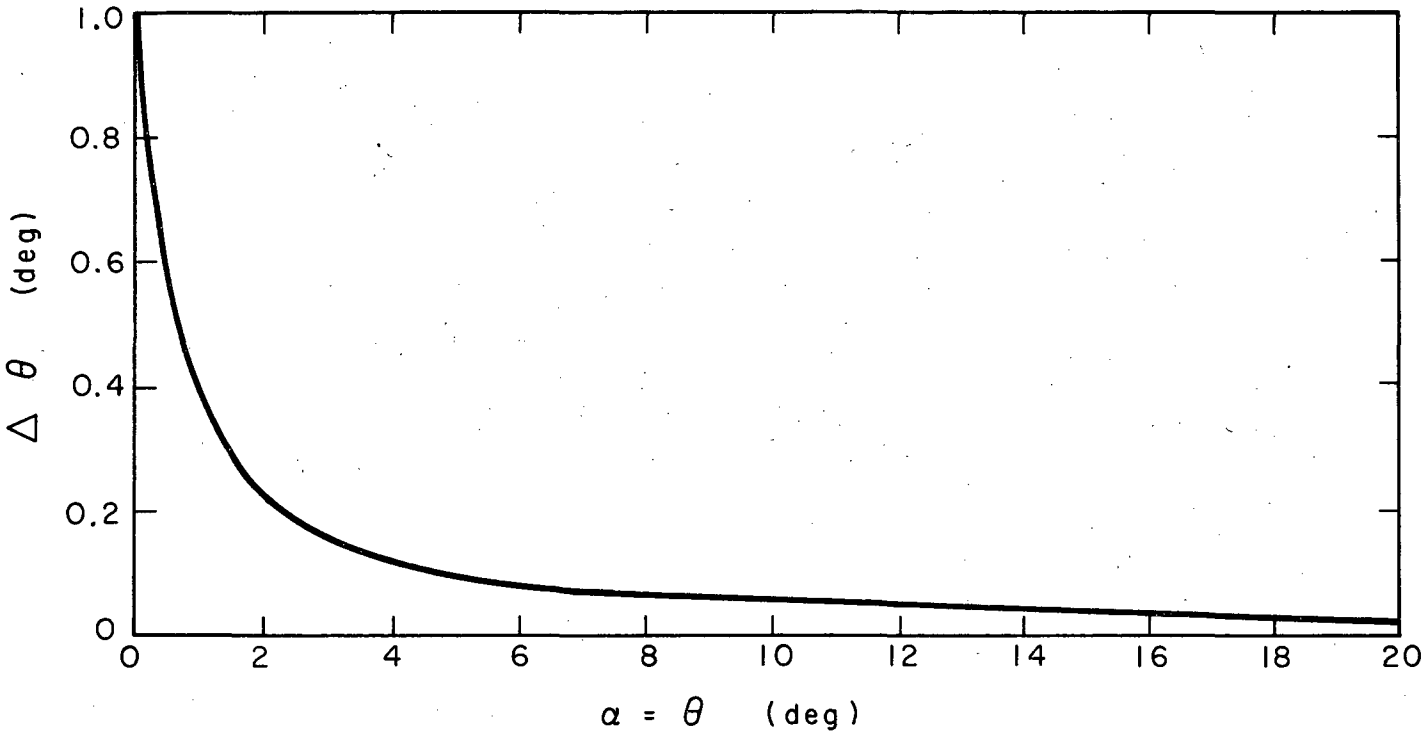

MUB-12751

Fig. 4. The change $\Delta\theta$ in scattering angle θ, as a function of the scattering angle α, for an angular spread in the vertical plane of $\Delta\rho = 1°$.

II. Individual Contributions to Energy Resolution

A. Beam Quality

A-1. Analyzed Beam

As was previously mentioned, it is necessary to analyze the extracted beam if good resolution is desired. For cave 1 at the 88" cyclotron, analysis is accomplished by bending the beam 57 degrees and subsequently separating the particles of different momenta with an analyzing slit which is placed at the horizontal focus (see Fig. 1, 2, 5).

Two particles whose momenta are p and $p+\Delta p$ will be bent through $\theta+\Delta\theta$ and θ respectively, where

$$\frac{\Delta p}{p} = \frac{\Delta\theta}{\theta} \qquad 3.$$

To obtain the energy spread we use the relation

$$p^2 = 2mE \; ; \qquad 4(a).$$

hence,

$$2p\Delta p = 2m\Delta E \qquad 4(b).$$

therefore,

$$\frac{\Delta E}{E} = \frac{2\Delta p}{p} = \frac{2\Delta\theta}{\theta} \qquad 5(a).$$

This equation implies that any degree of energy analysis is possible by narrowing the width of the analyzing slit. However, since the cyclotron source is not a point, particles of different momenta will overlap at the

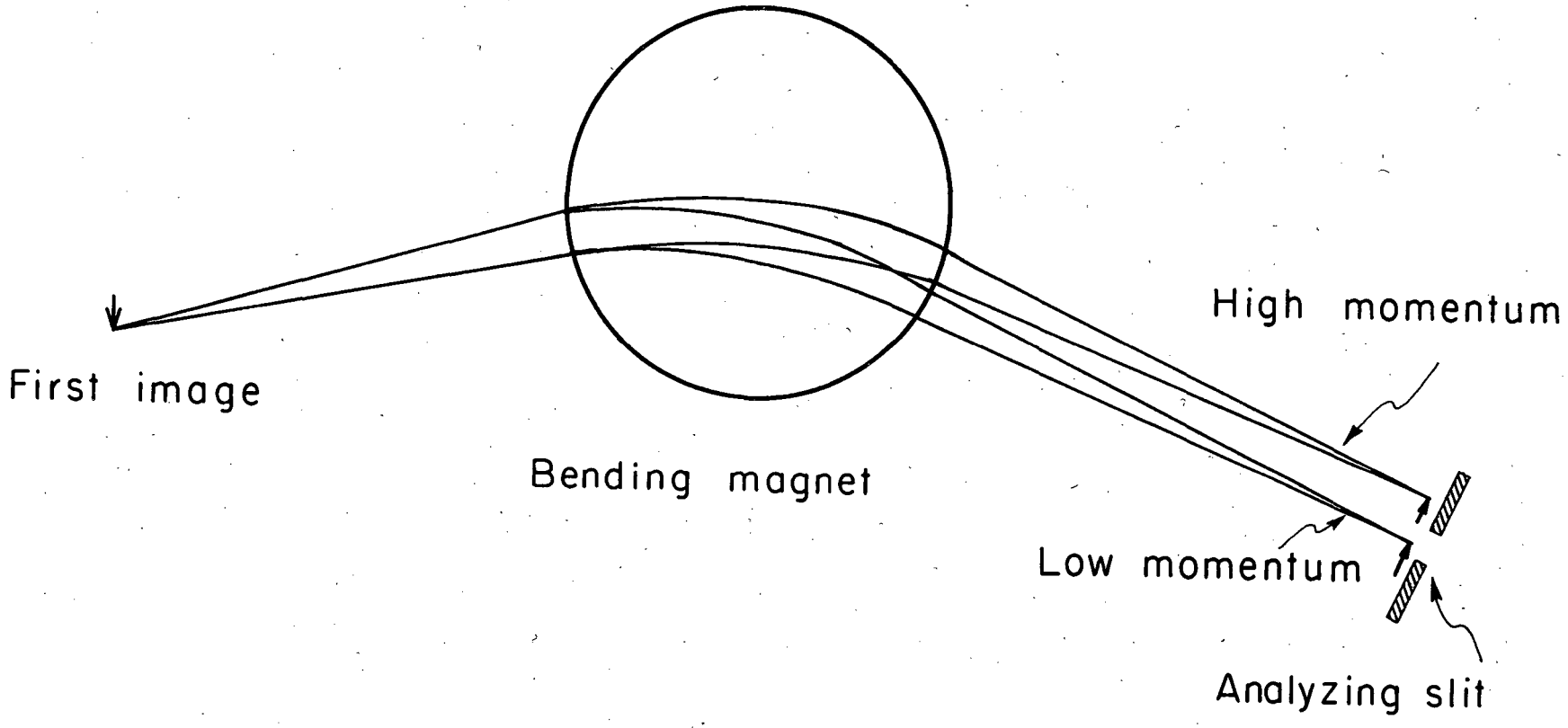

Fig. 5. An illustration of the effect of a finite source size on the energy resolution obtainable using a bending magnet.

MUB-12740

analyzing slit (see Fig. 5) and perfect separation is not possible. The optimum width of the analyzing slit is equal to the size of the image of the horizontal source at the slit. Closing the slit further will not improve the resolution of the beam but only reduce the beam intensity. From beam optics it has been calculated that the magnification from the source to the analyzing slit is 2.1. Since the width of the source is known to be .016", the image at the analyzing slit should be .034". Experimentally it is found that the beam resolution does not improve when the slit is closed beyond .040" to .060". From equation 5(a) we find that

$$\frac{\Delta E}{E} = \frac{\frac{2(.040 \text{ to } .060)}{147}}{1.0} = .054\% - .082\% \qquad 5(b).$$

where the distance from the center of the bending magnet to the analyzing slit is 147" (see Figs. 1, 2, 5). This is in reasonable agreement with the experimental value of $\frac{\Delta E}{E} = .07\%$. A more accurate calculation should include the effect of the fringing field of the cyclotron magnet (1, 3).

A-2. Beam Convergence

The angular divergence (in the horizontal plane) of particles emerging from the cyclotron effective source is about 1.9° full angle. To avoid scraping of the beam along the inside of the beam pipes, it is often necessary to reduce the divergence angle by means of a horizontal collimator (the "X"-collimator) close to the exit part of the cyclotron tank (see Fig.1,6). The angular divergence $\Delta\psi$ is given by

$$\tan \Delta\psi = \Delta\psi = \frac{x+s}{D} \qquad 6.$$

where x is the width of the "X" collimator, s is the source width and D is the distance from the source to the "X" collimator. If the magnification from the source to the center of the target chamber is M then the maximum angle of convergence at the target is

$$\Delta\psi_{BC} = \frac{x+s}{DM} \qquad 7.$$

If we assume that the cyclotron source uniformly illuminates the "X" collimator then the energy distribution due to beam convergence is rectangular with a width given by equation 7.

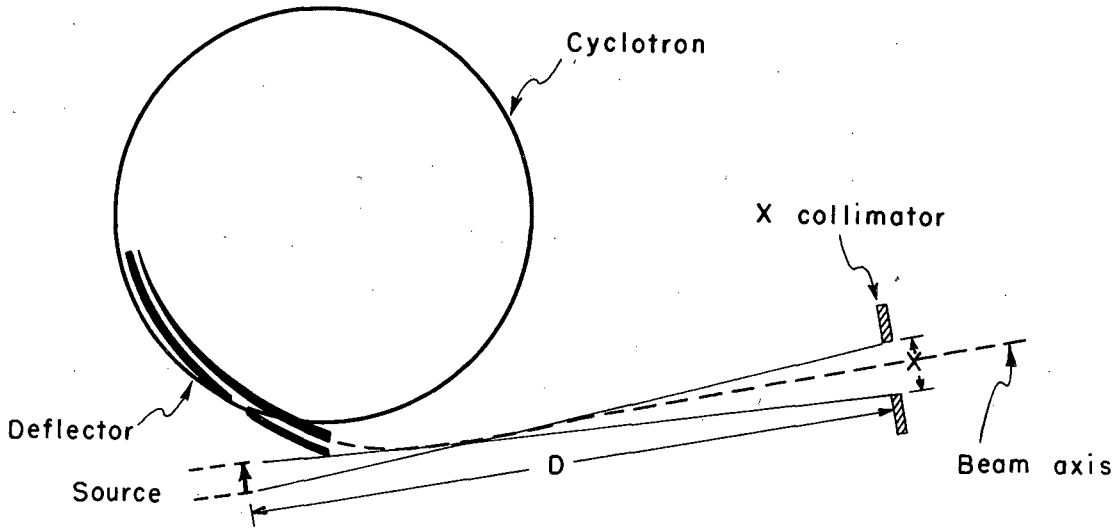

Fig. 6. Beam extraction system showing the effect of the "x" collimator on angular divengence.

A-3. Beam Width

A beam of finite width contributes an angular spread in the particles detected as shown in Fig. 7. For a given scattering angle θ_o, if CB $\ll$ L then

$$\Delta\psi_{BW} = \frac{CB}{L} \qquad 8.$$

but

$$CB=AB \sin(\theta_o+\phi) = \frac{W \sin(\theta_o+\phi)}{\sin \phi} \quad ; \qquad 9.$$

therefore,

$$\Delta\psi_{BW} = \frac{W}{L} \frac{\sin(\theta_o+\phi)}{\sin \phi} \qquad 10.$$

where W is the beam width, L is the distance from the target to the detector collimator and ϕ is the target angle measured with respect to the beam axis. The beam width may be determined if the width of the source and the magnification of the optical system are known, or it may be estimated from the size of the beam spot observed remotely. If we assume that the beam spot has a uniform density, then $\Delta\psi_{BW}$ produces a rectangular spread in energies with a width ΔE given by equations 1 and 10, provided that the reaction cross section is constant over the angle $\Delta\psi_{BW}$.

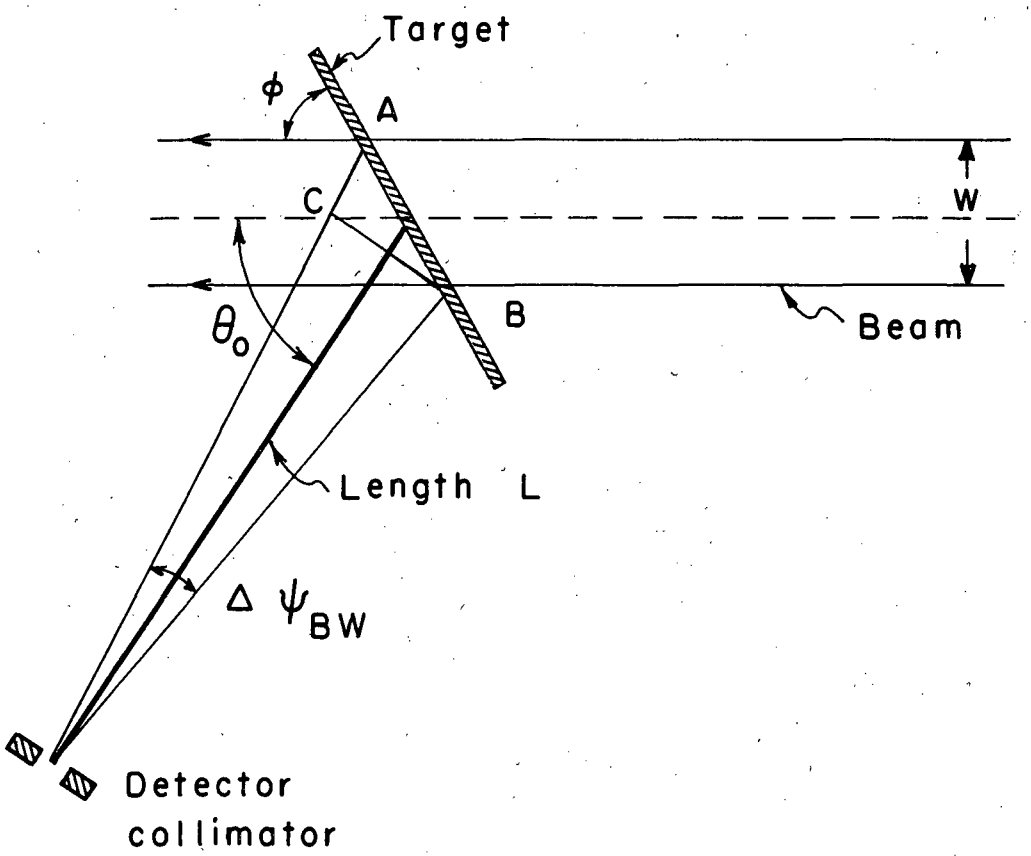

Fig. 7. The angular divergence $\Delta \psi_{B.W.}$ due to the physical width of the beam spot.

B. Target and Detector Geometry Effects

B-1. Solid Target

(a). Collimator Slit Width

If a solid target is used, the width of the detector collimator introduces an angular divergence which is easily calculated (see Fig. 8). For any scattering angle θ_o, if $L \gg C_R$, then

$$\Delta\psi_{csw} = \frac{C_R}{L} \quad , \tag{11.}$$

where C_R is the width of the detector collimator and L is the distance from the target to the collimator face. This divergence will have a rectangular shape provided the reaction cross section is constant over the angle $\Delta\psi_{csw}$.

(b). Target Thickness

The angular divergence due to reaction at different distances into the thickness of the solid target is very small. From Fig. 9, if $AC \ll L$, then

$$\Delta\psi_{TW} = \frac{AC}{L} \quad , \tag{12.}$$

but it can be seen that

$$AC = t' \sin\theta_o = t \frac{\sin\theta_o}{\sin\phi} \quad ; \tag{13.}$$

therefore,

$$\Delta\psi_{TW} = \frac{t}{L} \frac{\sin\theta_o}{\sin\phi} \quad , \tag{14.}$$

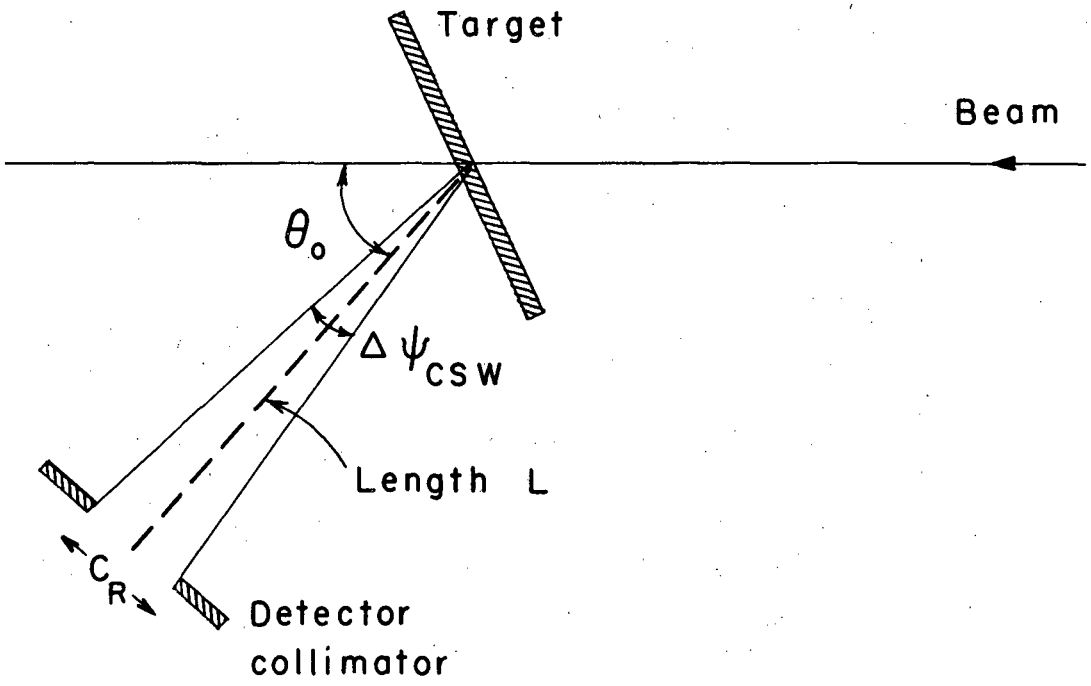

Fig. 8. The angular divergence for a solid target due to the detector collimator slit width.

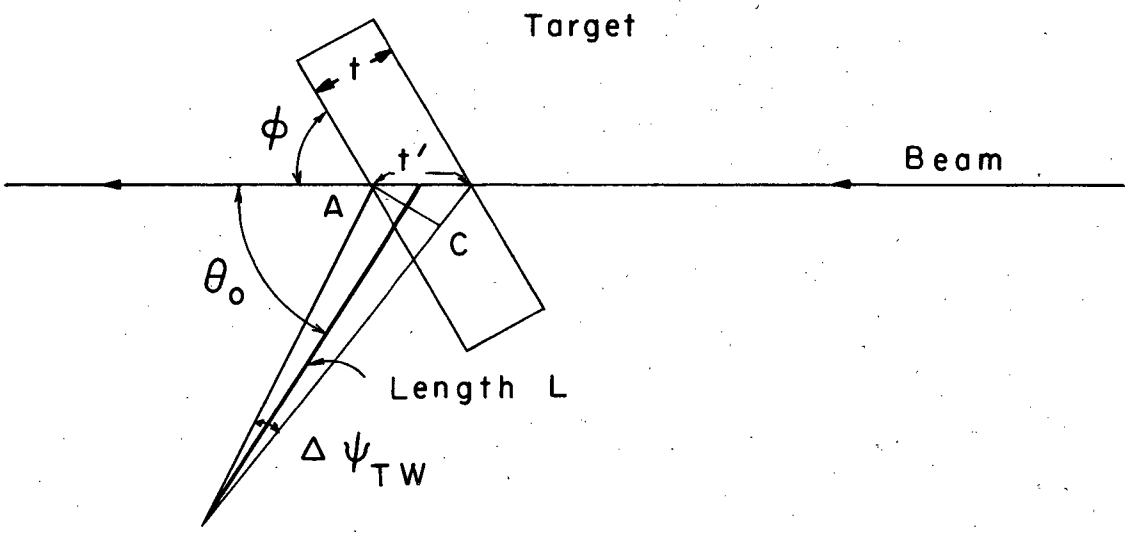

Fig. 9. The angular divergence for a solid target due to the thickness of the target.

where t is the target thickness and ϕ is the target angle with respect to the beam axis. A comparison with equation 10 for $\sin\theta_o/\sin\phi = 1$, indicates that this effect is negligible since $C_R \gg t$. Of course there are more serious effects, discussed below, due to multiple scattering and energy straggling in thick targets.

B-2. Gas Target Collimator Slit Widths

In a gas target experiment it is necessary to use two detector collimators. We will consider the case when the collimators are of equal width. This geometry is required for the cross section formula most commonly used.

If we assume a scattering angle $\theta_o = 90°$, then the intensity of particles scattering through any angle θ (see Fig. 10) is proportional to length I. This length represents the number of centers along the incident beam which can scatter particles at an angle θ such that they will pass through both collimators. For $\theta = \theta_o - \Delta\theta$

$$\tan\Delta\theta = \Delta\theta = \frac{C_R - I}{(L-L_f)} \quad ; \qquad 15.$$

therefore,

$$I = C_R - (L-L_f)\Delta\theta \quad , \qquad 16.$$

where C_R is the width of the collimators and $L-L_f$ is the distance between them. A plot of intensity as a function of scattering angle (at a fixed θ_o) is shown in Fig. 11. The effective angular divergence is triangular in shape with a full width at half maximum (FWHM) of $\frac{Cr}{L-L_f}$.

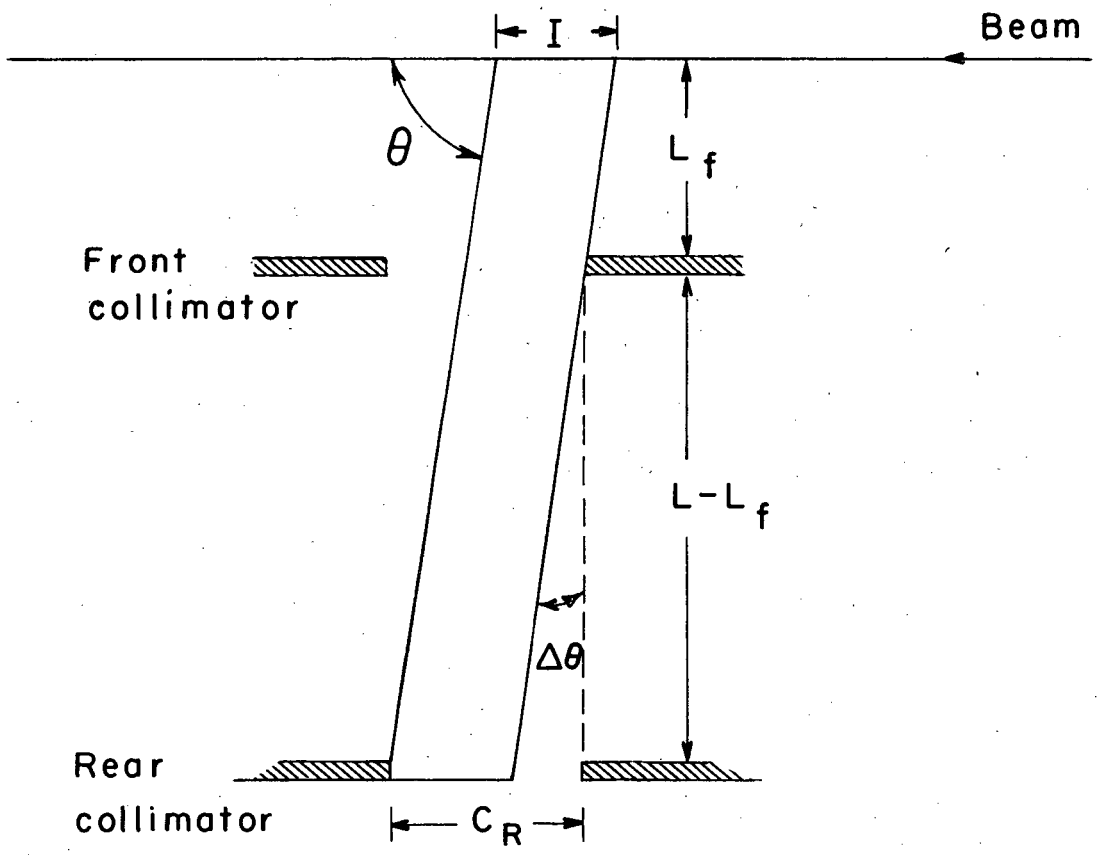

Fig. 10. The angular divergence for a gas target due to the width of detector collimators.

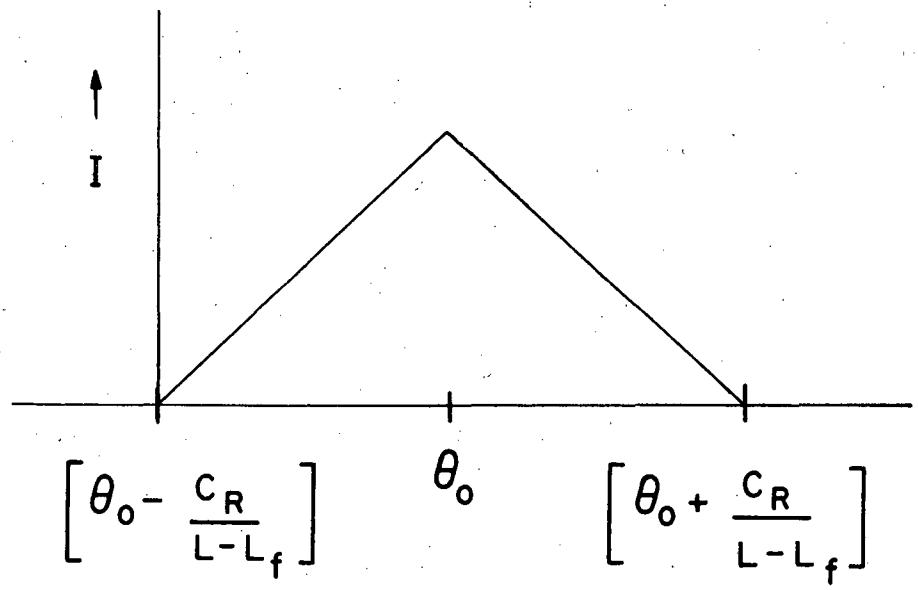

MUB-12750

Fig. 11. The intensity of particles (I) observed using a gas target collimator system as, a function of the scattering angle θ, for some mean scattering angle θ_o.

If $\Delta\theta$ is small it can be shown that equation 16 holds for any scattering angle θ_o.

C. Energy Straggling

Charged particles passing through matter lose energy primarily by collisions with atomic electrons. Because of statistical fluctuations in the number of collisions a monoenergetic beam will be spread in energy after passing through an absorber. The absorber may be a thin detector used for determining a differential energy loss, or a target. In the latter case the energy spread contributes to the total resolution observed.

The distribution of energies is approximately gaussian but nuclear collisions give it a "tail" on the side of greater energy loss. We have neglected this asymmetry in our applications. An expression derived by Bohr[4] permits estimation of the magnitude of the effect and displays the approximate dependence of the FWHM on several variables. The FWHM of the gaussian distribution is

$$\Delta E(\text{FWHM}) = 1.66\left(\frac{8\pi z^2 e^4 A_n t Z}{A}\right)^{1/2} \qquad 17(a).$$

where t is the target thickness in g/cm^2, A_n is Avogadros number, A is the atomic weight of the target, z and Z are the nuclear charges of the incoming particle and the target nucleus respectively, and e is the unit electronic charge. Substituting the numerical values of the constants equation 17a simplifies to

$$\Delta E = 29.4\ z\left(\frac{Z}{A}t\right)^{1/2} \qquad 17(b).$$

where t is now in mg/cm^2 and E is in keV. Note that the FWHM is independent of beam energy (to this approximation) and since $Z/A \simeq 1/2$ for all elements, it is approximately independent of target material.

A more accurate method of calculating energy distributions for charged particle beams passing through absorbers has been given by Symon[5]. His work is conveniently summarized by Kraft, Mangelson, and Rogers[6]. The latter reference gives all formulas and graphs necessary for calculating energy straggling distributions at cyclotron energies, as well as some specific applications.

D. Multiple Scattering

When charged particles pass through thin absorbers they undergo several small-angle coulomb deflections randomly oriented such that the overall distribution of angles is gaussian to first order. This simple theory of multiple scattering[7] predicts that the mean square scattering angle $\langle\theta^2\rangle$ is given by

$$\langle\theta^2\rangle = k \ln \frac{k}{(\theta \text{ min})^2} \qquad 18.$$

where

$$k = \frac{4\pi A_n t Z(Z+1) z^2 e^4}{A p^2 v^2} ,$$

p and v are the momentum and velocity of the incoming particle respectively and the other terms are as defined previously.

In the classical limit where $\gamma = \frac{Zze^2}{\hbar v} > 1$,

$$\theta \text{ min} = \frac{\gamma \hbar Z^{1/3}}{p a_o} \qquad 19.$$

where a_o is the Bohr radius. In this case $\langle \theta^2 \rangle$ simplifies to

$$\langle \theta^2 \rangle = 3.93 \times 10^{-2} \frac{Z^2 z^2 t}{AE^2} \log \frac{2.12 \times 10^8 t}{AZ^{2/3}} \qquad 20.$$

When $\gamma \ll 1$, in the limit of the Born approximation, $\theta \text{ min} = \frac{\hbar}{pa_o} Z^{1/3}$. If $\gamma \simeq 1$, as for 22 MeV protons on copper, neither approximation is valid and it is necessary to use the more complete treatment of Moliere[8] which takes into account single scattering and the transition from single scattering to multiple scattering. J. B. Ball[9] has performed these calculations at several energies for a number of different incident particles and targets. When $\gamma \gg 1$ equation 20 is in good agreement with Ball's calculation. However, for $\gamma \approx 1$, they deviate by 20% or more.

Although inaccurate in certain cases, the simple theory does illustrate some of the important functional relationships of multiple scattering. For solid targets of 1 mg/cm^2 or less, multiple scattering is usually only a small contribution to the total angular resolution. However, this is generally not the case for gas targets since the window thickness must be taken into account.

E. Electronic Noise

The factors contributing to electronic noise in experiments with semiconductor detectors has recently been reviewed by F. S. Goulding[10]. Experimentally the contribution from electronic noise can easily be measured with a calibrated pulser.

III. Combination of Sources of Energy Spread

To properly combine two energy distributions one must solve the fold or convolution integral

$$f(t) = \int g(x)h(t-x)dx \qquad 21.$$

at every point that the resultant distribution is desired[11]. In equation 21 g(x) and h(x) are the functional forms of the original energy distributions. This equation is applicable only to distributions which are uncorrelated. This criterion is met to a very good approximation by all distributions considered here.

Frequently g(x) and h(x) are gaussians in which case f(t) is also gaussian with a FWHM given by

$$\Delta E_f = \sqrt{(\Delta E_g)^2 + (\Delta E_h)^2} \qquad 22.$$

When non-gaussian distributions are combined, equation 21 must be solved at several points to determine f(t). The use of equation 21 is illustrated in Fig. 12 where the beam width and beam convergence distributions are combined.

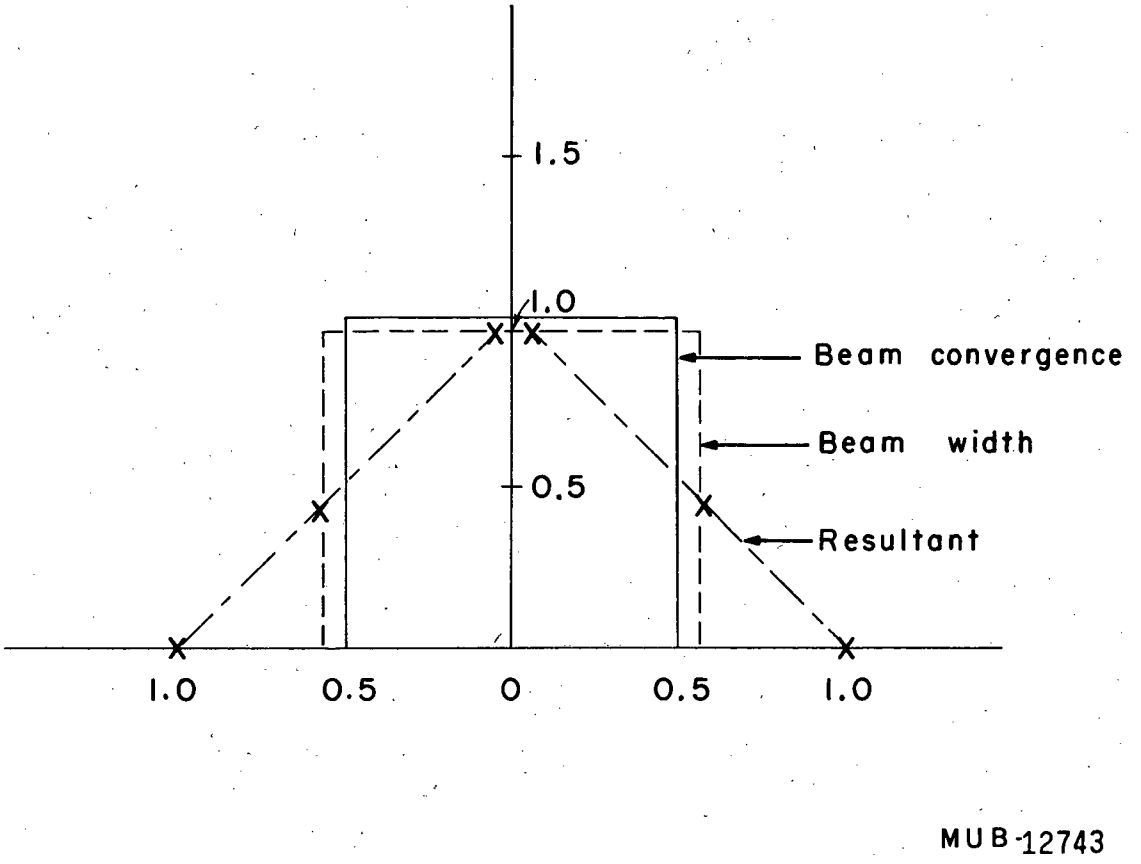

Fig. 12. The beam convergence distribution (calculated from equation 7) and the beam width distribution (calculated from equation 10) were folded using equation 21. The resultant (f(t)) was determined at the points marked X.

It is convenient to normalize g(x) and h(x) to unit area. This insures that f(t) will be properly normalized (unit area).

Folding gaussian and non-gaussian distributions together is more difficult. However we have found that combination of all non-gaussian (rectangular) distributions frequently produces a resultant which is well represented by a gaussian. This is a very good approximation when three or more rectangular distributions of approximately equal FWHM are combined as is illustrated in Fig. 13.

IV. Theoretical Applications to Experimental Results

The theory outlined in the previous sections has been applied to the scattering of 50.7 MeV alpha particles from ^{1}H, ^{12}C and ^{197}Au. Tables 4-7 summarize the results.

Alpha particles scattered by hydrogen in a mylar ($C_{10}H_8O_4$) target produce a very broad gaussian peak. The width of the peak is almost completely determined by the angular resolution since $\left(\frac{dE}{d\theta}\right)$ is very large. The resultant $\Delta\psi$ (FWHM) can then be determined by dividing the width of the observed peak by $\left(\frac{dE}{d\theta}\right)$. The experimental results are shown in Table 4. Neglecting a small change in $\sin\theta_o$ (see equation 10), $\Delta\psi$ should be constant at all three angles.

The individual angular effects contributing to the width of the experimental peak were calculated using the equations given in section II (see Table 5). The distributions were then combined, using equation 21, to give the resultant theoretical $\Delta\psi$ (see Table 5).

The resolution for alpha particles elastically scattered by gold is primarily determined by the energy spread of the analyzed beam, the electronic noise, and

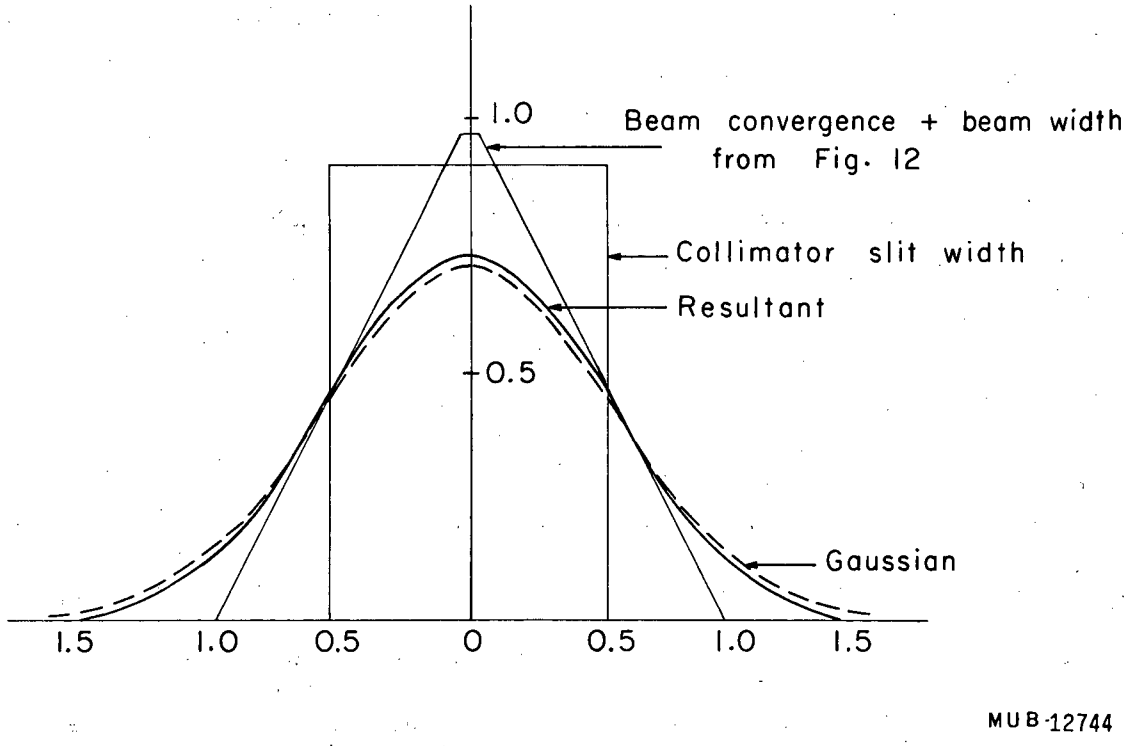

Fig. 13. The trapezoidal resultant from figure 12 was folded with the collimator slit distribution, using equation 21, to give the new resultant. A gaussian with the same FWHM as the folded distribution is shown for comparison.

energy straggling in the target. The contribution from electronic noise was measured using a calibrated pulser and energy straggling was calculated using equation 17. In this way the analyzed beam was determined to be .11% using equation 22 (see Table 6).

The resolution for alpha particles scattered by C^{12} is sensitive to both angular dependent and angular independent effects. In Table 7 the theoretical and experimental energy resolutions are compared for scattering angles from 11 to 46 degrees. Although $\frac{dE}{d\theta}$ and $\Delta\psi$ vary widely over this region, good agreement with experimental results was obtained (see Table 7).

Acknowledgment

The authors would like to express their appreciation to Dr. Bernard Harvey and Professor Joseph Cerny for suggesting this project and for many helpful discussions. We would also like to acknowledge the assistance of Hank Brunnader, Creve Maples and Don Fleming.

TABLE 2

$^{1}H(\alpha,\alpha')^{1}H$

E_{α} = 50.7 MeV

Lab Angle (Deg)	CM Angle (Deg)	Particle Energy (MeV)
+ 1	50.01	50.638
+ 2	10.02	50.452
+ 3	15.07	50.141
+ 4	20.19	49.702
+ 5	25.38	49.132
+ 6	30.68	48.426
+ 7	36.13	47.577
+ 8	41.76	46.573
+ 9	47.64	45.400
+10	53.85	44.035
+11	60.54	42.439
+12	67.95	40.543

TABLE 3

$^{12}C(\alpha,\alpha)^{12}C$

E_α = 50.7 MeV

Lab Angle (Deg)	CM Angle (Deg)	Particle Energy (MeV)
+ 2	2.671	50.679
+ 4	5.342	50.617
+ 6	8.011	50.513
+ 8	10.67	50.369
+10	13.34	50.184
+12	16.00	49.960
+14	18.65	49.696
+16	21.31	49.395
+18	23.95	49.056
+20	26.59	48.681
+22	29.22	48.271
+24	31.84	47.827
+26	34.46	47.351
+28	37.06	46.844
+30	39.66	46.308
+32	42.24	45.744
+34	44.81	45.154
+36	47.37	44.540
+38	49.92	43.904
+40	52.45	43.247

TABLE 4

50.7 MeV Alpha Particles Scattered by Hydrogen

Lab Angle (deg.)	Experimental ΔE (keV)	$(\frac{dE}{d\theta})$ (keV/deg)	Experimental $\Delta\psi$(deg)
7	352	931	.378
9	503	1273	.395
11	678	1947	.388
		Average	.387

TABLE 5

Theoretical Angular Resolution at 9° for scattering of 50.7 MeV Alpha Particles by Hydrogen

	Distribution Shape	$\Delta\psi$(deg)
Beam Convergence	Rectangular	.094
Beam Width	Rectangular	.308
Collimator Width	Rectangular	.268
Multiple Scattering	Gaussian	.139

Combined Theoretical	$\Delta\psi$(deg)	=	.390 deg
Experimental	$\Delta\psi$(deg)	=	.387 deg

TABLE 6

50.7 MeV Alpha Particles Scattered by ^{197}Au

Lab Angle	Experimental ΔE (FWHM)	Pulser (FWHM)	Energy Straggling
16°	67.6 keV	33.6 keV	14.6 keV
18°	68.9 "	"	"
20°	66.3 "	"	"
22°	67.2 "	"	"

Analyzed beam was determined to be 57 keV or .11%

TABLE 7

50.7 MeV Alpha Particles Scattered by ^{12}C

Lab Angle (deg)	Theoretical $\Delta\psi$(deg)	$(\frac{dE}{d\theta})_{\theta o}$ (keV/deg)	$(\frac{dE}{d\theta})_{\theta o} \Delta\psi$(keV)	Energy Straggling (keV)	Electronic Noise (keV)	Analyzed Beam (keV)	ΔE(FWHM) Theoretical (keV)	ΔE(FWHM) Observed (keV)
11	.372	110	41	26.4	33.6	56.8	82	82
22	.352	210	74				103	106
30	.333	271	90.3				115	112
38	.306	319	97.6				121	126
46	.284	370	105				127	130

References

1. B. G. Harvey, E. J-M. Rivet, A. Springer, J. R. Meriwether, W. B. Jones, J. H. Elliott and P. Darriulat, Nucl. Phys. 52, 465 (1963).
2. John J. Livingood, Principles of Cyclic Particle Accelerators, D. Van Nostrand Company, Inc. Princeton, New Jersey, 1963.
3. Bernard G. Harvey, unpublished Magnet Notes.
4. Emilio Segre, Nuclei and Particles, W. A. Benjamin, Inc., New York, 1964.
5. K. R. Symon, Fluctuations in Energy Lost by High Energy Charged Particles in Passing Through Matter, Thesis, Harvard University, 1948.
6. Mary Kraft, Nolan Mangelson, and George Rogers, Lawrence Radiation Laboratory Report, UCRL-11602, 1964.
7. E. Segre, Ed., Experimental Nuclear Physics, Vol. 1, John Wiley and Sons, Inc., New York, 1953.
8. G. Moliere, Z. Naturforsch 3a, 78, 1948.
9. J. B. Ball, Oak Ridge National Laboratory Report, ORNL-3311, 1963.
10. Fred S. Goulding, Lawrence Radiation Laboratory Report, UCRL-16231, 1965.
11. H. J. Longley, Los Alamos Scientific Laboratory, LA-2729, 1962.

This report was prepared as an account of Government sponsored work. Neither the United States, nor the Commission, nor any person acting on behalf of the Commission:

A. Makes any warranty or representation, expressed or implied, with respect to the accuracy, completeness, or usefulness of the information contained in this report, or that the use of any information, apparatus, method, or process disclosed in this report may not infringe privately owned rights; or

B. Assumes any liabilities with respect to the use of, or for damages resulting from the use of any information, apparatus, method, or process disclosed in this report.

As used in the above, "person acting on behalf of the Commission" includes any employee or contractor of the Commission, or employee of such contractor, to the extent that such employee or contractor of the Commission, or employee of such contractor prepares, disseminates, or provides access to, any information pursuant to his employment or contract with the Commission, or his employment with such contractor.